F. Méot
DAPNIA & IN2P3

6-D simulation of spiral FFAG

Contents

1 Introduction

Main goals of the work presented :

• Achieve 3-D simulation of the field in an spiral FFAG magnet, from just its geometrical parameters.

The method is derived from former radial FFAG triplet simulation kit [see FFAG04, KEK].

• Application to 6-D tracking : from properties properties to DA, transmission efficiency, etc.
- for RACCAM project
- muon
- and other proton driver

Various outcomes of these spiral magnet simulations :

• They provide
(i) analytical 3-dimensional field modeling ("`FFAGSPI`"),
(ii) possibility of ultra-fast generation of field maps ("`POLARMES`").

• they yield fast, high precision multi-turn tracking

• they allow fast approach, *prior to, or in parallel with 3-D magnet code use*, to optimization of magnet geometry using the built-in matching procedures ("`FIT`").

2 Ingredients necessary for magnet simulation

They are the ingredients that go into the Taylor developement of equations of motion :

$$\bullet Position \ : \ \vec{R}(M_1) \approx \vec{R}(M_0) + \vec{u}(M_0)\,\Delta s + \vec{u}'(M_0)\,\frac{\Delta s^2}{2!} + ... + \vec{u}''''''(M_0)\,\frac{\Delta s^6}{6!} \ [+...] \quad (1)$$

$$\bullet Velocity \ : \ \vec{u}(M_1) \approx \vec{u}(M_0) + \vec{u}'(M_0)\,\Delta s + \vec{u}''(M_0)\,\frac{\Delta s^2}{2!} + ... + \vec{u}''''''(M_0)\,\frac{\Delta s^5}{5!} \ [+...]$$

using $\vec{u}' = \vec{u} \times \vec{B}$ (**Lorentz equation**), $\vec{u}'' = \vec{u}' \times \vec{B} + \vec{u} \times \vec{B}'$, $\vec{u}''' = ...$ *etc.*

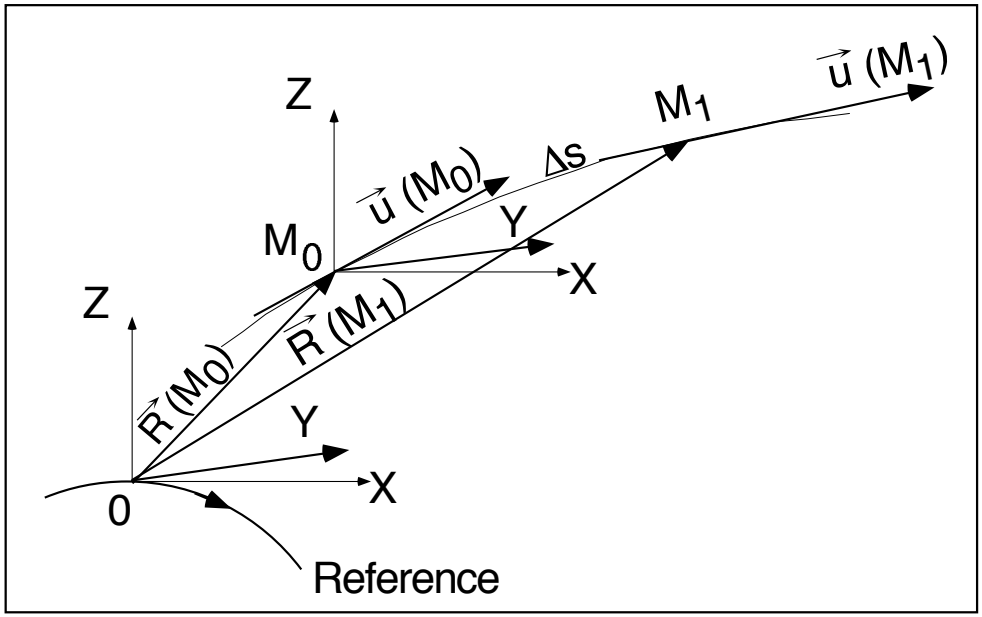

Figure 1: **Position and velocity of a particle in the reference frame.**

Note : if spin tracking (muon !), then in addition

$$\bullet \ \vec{S}(M_1) \approx \vec{S}(M_0) + \vec{S}'(M_0)\,\Delta s + ... + S''''(M_0)\frac{\Delta s^4}{4!} \ [+...] \quad \textbf{using} \ \vec{S}' = \vec{S} \times \Omega(\vec{u}, \vec{B}), \ \vec{S}'' = ... \ etc. \quad (2)$$

Taylor coefficients

Four steps are necessary to calculate $\boxed{\vec{B}(s)}$ **and its derivatives** $\boxed{d^n\vec{B}/ds^n}$ **:**

1. **Mid-plane field model of the FFAG form** $\boxed{B_z(r,\theta) = B_{z0}\,\mathcal{F}(r,\theta)\,\mathcal{R}(r)}$
   from what derivatives will further be drawn : $\partial^{i+j}B_z/\partial\theta^i\partial r^j$

2. **Next, transform from magnet cylindrical frame into Zgoubi Cartesian frame, using**

$$\partial B_z/\partial X = (1/r)\partial B_z/\partial\theta, \quad \partial B_z/\partial Y = \partial B_z/\partial r, \quad \partial^2 B_z/\partial X^2 = (1/r^2)\partial^2 B_z/\partial\theta^2 + (1/r)\partial B_z/\partial r, \quad etc.$$

3. Z**-derivatives and extrapolation off mid-plane yield the 3-D** $\vec{B}$ **model**

$$\boxed{\vec{B}(X,Y,Z), \qquad \partial^{i+j+k}\vec{B}/\partial X^i\partial Y^j\partial Z^k}$$

4. **Eventually, the derivatives** $\boxed{d^n\vec{B}/ds^n}$ **needed in Eqs. 1 are derived from the above using**

$$\vec{B}'(s) = \sum_i \frac{\partial\vec{B}(X,Y,Z)}{\partial X_i}\,u_i(s)\,, \qquad \vec{B}''(s) = \sum_{ij} \frac{\partial^2\vec{B}(X,Y,Z)}{\partial X_i\partial X_j}\,u_i(s)\,u_j(s) + \sum_i \frac{\partial\vec{B}(X,Y,Z)}{\partial X_i}\,u_i'(s) \quad etc.$$

($X_{i,j,...}$, $i,j,... = 1,3$ stand for X, Y or Z).

3 Spiral FFAG magnet

Reminder : former N-tuple radial FFAG magnet procedure [FFAG04]

GEOMETRY/EFBs FOR ONE DIPOLE :

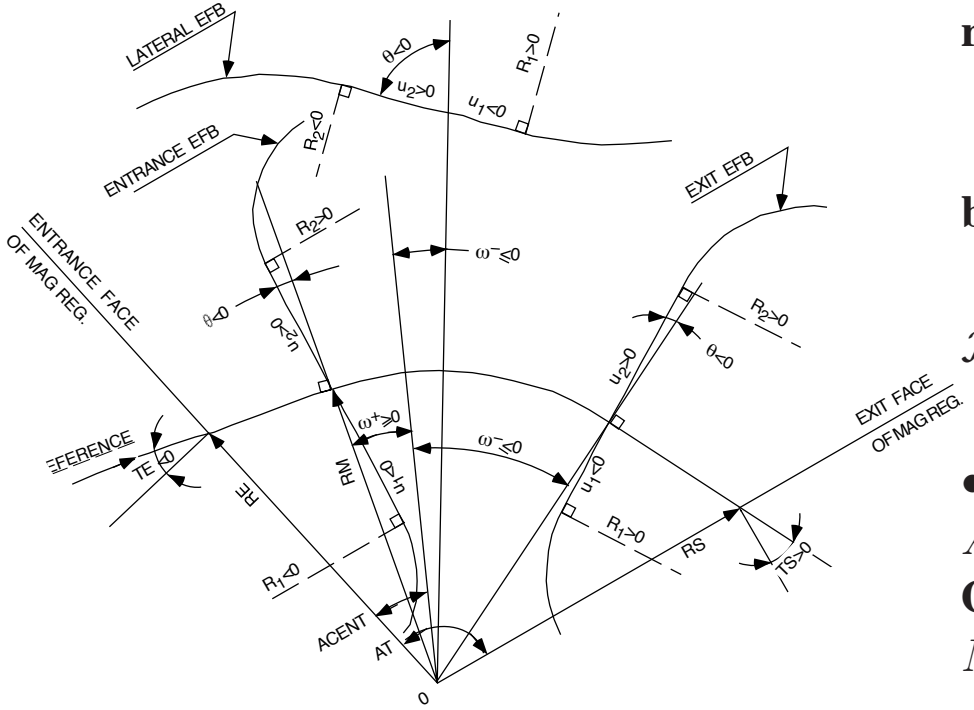

GEOMETRY/EFBs FOR A RADIAL TRIPLET :

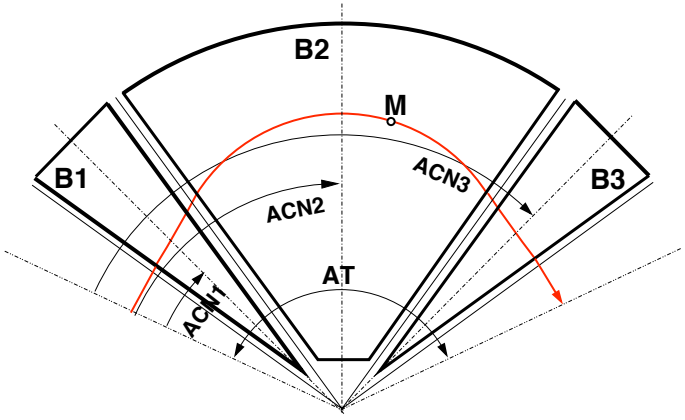

• **If alone - at the left - a dipole is encompassed in the lim iting region defined by the angle AT. The dipole geomet rical parameters yield the mid-plane orthogonal field :**

$$B_{zi}(r,\theta) = B_{z0,i}\,\mathcal{F}_i(r,\theta)\,\mathcal{R}_i(r)$$

by using

$$\mathcal{R}_i(r) = (r/R_{0,i})^K$$

$$\mathcal{F}_i(r,\theta) = \mathcal{F}_{\mathbf{EFBin}}(r,\theta)\times\mathcal{F}_{\mathbf{EFBout}}(r,\theta)\times\mathcal{F}_{\mathbf{EFBorder}}(r,$$

• **A N-tuple ($N = 3$) will be encompassed as well withi AT. The individuals dipoles are positioned by $ACNi$'s. Obtaining the total field is a matter of summing over th N neighboring dipoles :**

$$B_z(r,\theta) = \sum_{i=1}^{N} B_{zi}(r,\theta) = \sum_{i=1}^{N} B_{z0,i}\,\mathcal{F}_i(r,\theta)\,\mathcal{R}_i(r)$$

Derivatives : $$\frac{\partial^{i+j}\vec{B}_z(r,\theta)}{\partial\theta^i\partial r^j} = \sum_{i=1,N}\frac{\partial^{i+j}\vec{B}_{zi}(r,\theta)}{\partial\theta^i\partial r^j}$$

Note : **this is a "trick", not necessarily true linear super position**

Spiral FFAG magnet

A GEOMETRY THAT INCLUDES FIELD CLAMPS :

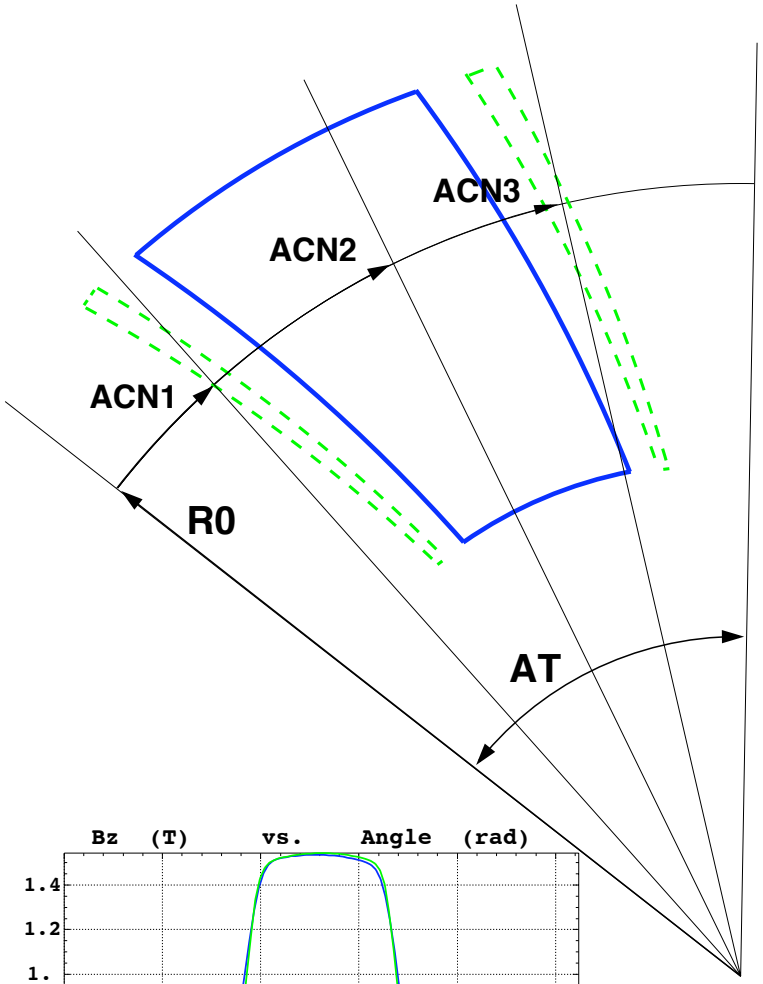

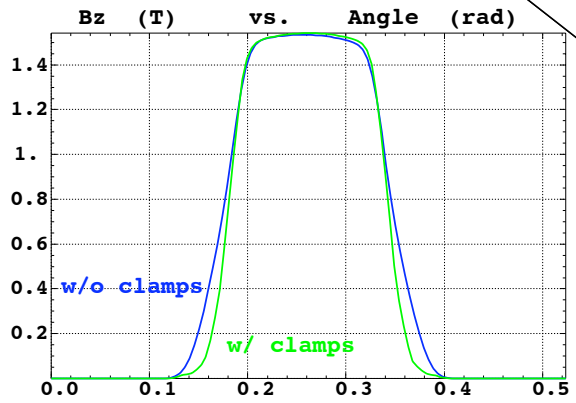

We maintain the "N-tuple" modeling.
Underlying goal, here : introducing some non-zero B in clamps will allow simulating their (normally passive) effect.

• Analytical model, for each one ("i" index) of the sectors - at the left :

$$B_{zi}(r,\theta) = B_{z0,i}\,\mathcal{F}_i(r,\theta)\,\mathcal{R}_i(r)$$

$$\mathcal{R}_i(r) = (r/R_{0,i})^K$$

• For each one of these 3 sectors :

$$\mathcal{F}_i(r,\theta) = \mathcal{F}_{\textbf{EFBin}}(r,\theta)\times\mathcal{F}_{\textbf{EFBout}}(r,\theta)\times\mathcal{F}_{\textbf{EFBorder}}(r,\theta)$$

Calculation of the $\mathcal{F}_{\text{EFB}}$'s $\longrightarrow$ discussed next slide.

• Overall field, given N neighboring sectors :

$$B_z(r,\theta) = \sum_{i=1}^{N} B_{zi}(r,\theta) = \sum_{i=1}^{N} B_{z0,i}\,\mathcal{F}_i(r,\theta)\,\mathcal{R}_i(r)$$

Simulation of field fall-offs

Field fall-off at an *EFB* (*EFBin*, *EFBout*, *EFBorder*) is modeled by

$$\mathcal{F}_{EFB}(d) = (1+\exp[P(d)])^{-1}\,, \quad P(d) = C_0 + C_1\frac{d}{g} + C_2\left(\frac{d}{g}\right)^2 + \ \ldots\ + C_5\left(\frac{d}{g}\right)^5$$

- $d \equiv d(r,\theta)$ **is the distance to the spiral** *EFB*.
  Computed by Newton method : "the normal to the spiral at (x_n, y_n) **contains the observation point** (x_b, y_b)**)" :**

```
theta=RTNEWT(xb,yb,d,a,amin,amax,xacc,ttarf)
xn = d*exp(a*theta)*cos(theta+thetaref)
yn = d*exp(a*theta)*sin(theta+thetaref)
d=sqrt( (xb - xn)**2 + (yb - yn)**2 )
```

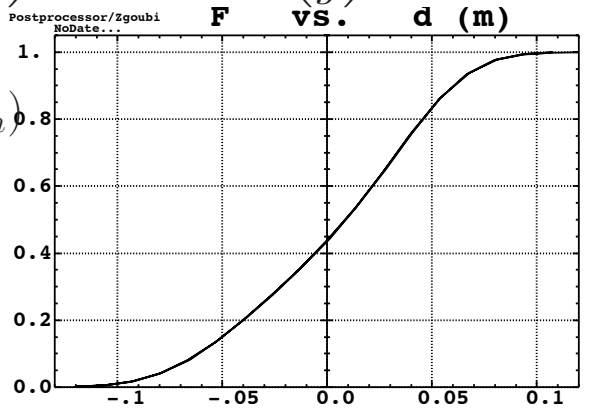

Figure 2: Gap $g = 8$ cm, $C_0 = 0.1455$, $C_1 = 2.2670$, $C_2 = -0.6395$, $C_3 = 1.1558$, $C_4 = C_5 = 0$.

- $\mathcal{F}_{EFB}(d)$ **accounts for gap shape :**

  $g(r) = g_0(R_0/r)^K$ **(pole shaping),**
  or
  $g = C^{\underline{\mathbf{st}}}$ **(parallel gap, coil shaping)**
  or
  $g = g_0\, r/R_0$ **(coil shaping** $\rightarrow$ $C^{\underline{\mathbf{st}}}$ **vertical tune)**

- $C_0 - C_5$ **coefficients determine the shape of field fall-off**
  (can be computed from prior POISSON or TOSCA runs)

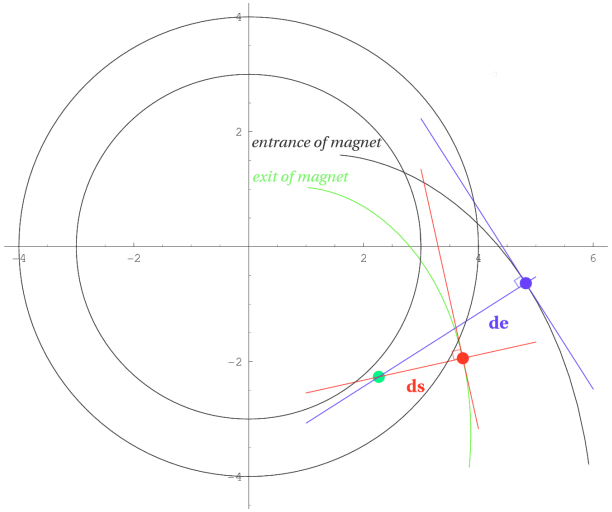

Calculation of the mid-plane field and its derivatives

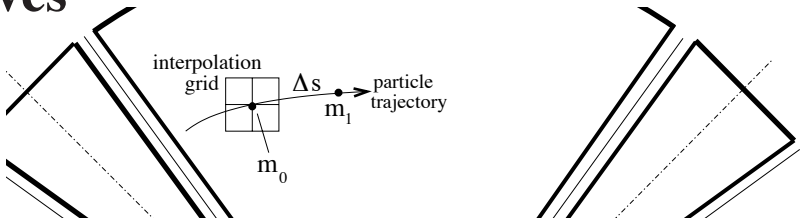

Two different methods have been implemented, based on

• (i) numerical interpolation from a "flying mesh".
In this case $B_z(r, \theta, Z = 0)$ is computed at the $n * n$ nodes ($n = 3$ or 5 in practice) of a "flying" interpolation mesh centered on the actual $(r, \theta, Z = 0)$ particle position projection.

• (ii) construction of a 2-D mid-plane magnetic field map.

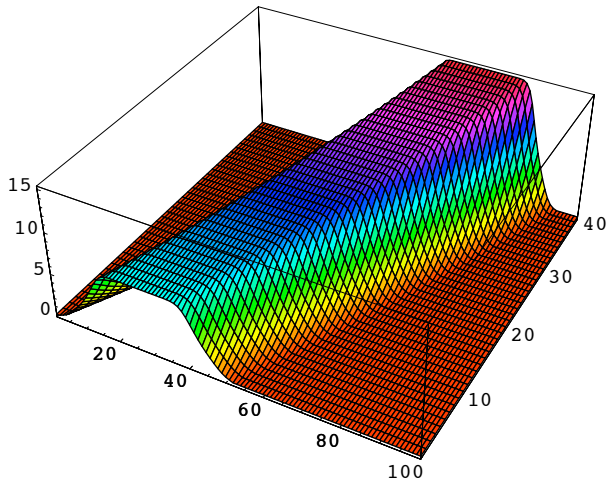

In this case the $n * n$ nodes are taken closest to particle position, at each integration step.

• (iii) a third method is under installation : analytical expressions of $B_z(r, \theta, Z)$ and derivatives $\partial^{i+j+k}/\partial r^i \partial \theta^j \partial z^k$.

- The first method has the merit of facilitating easy possible changes to the source code so as to modify the mid-plane magnetic field model $B_z(r, \theta)$.
In addition it allows parameter optimization using "FIT".

- The second method has the merit of faster tracking.

- Both methods feature excellent symplecticity - dependent upon, (i) mesh size, (ii) integration step size.

- The third methods has all the merits, speed, symplecticity, "FIT" compliant.

4 Numerical results

4.1 Field along closed orbits :

$$B_z(r,\theta) = B_{z0}\,\mathcal{F}(r,\theta)\,\mathcal{R}(r) \text{ at } r = r_{\mathbf{co}}(\theta)$$

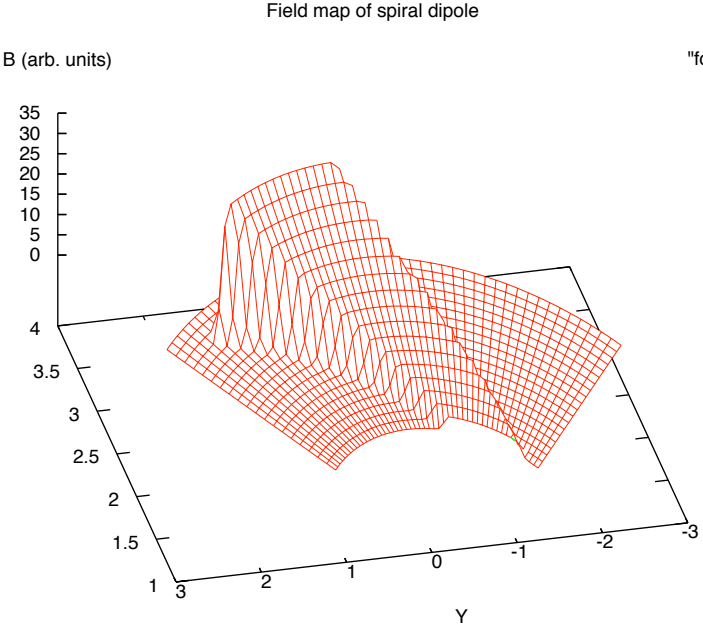

Typical geometry considered :

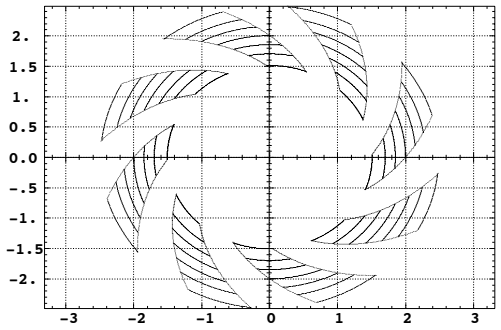

8 cell ring
$r_{\mathbf{min}}$ = 1.5 m
$r_{\mathbf{max}}$ = 2.5 m
spiral angle ξ = 52 degrees
K = 2.5

MID-PLANE FIELD, g=4 cm

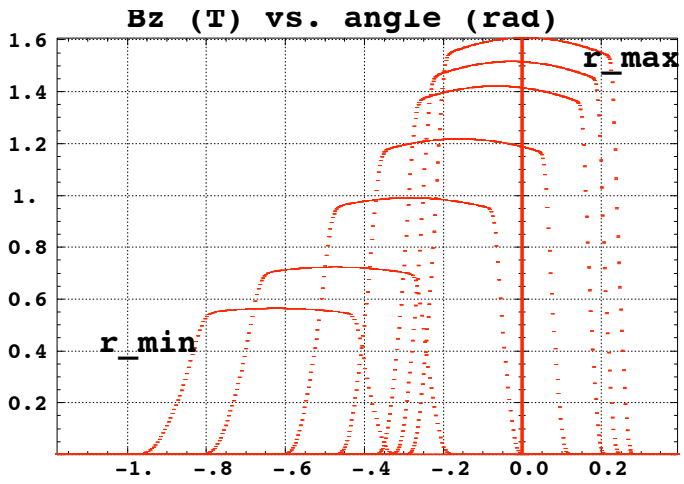

MID-PLANE FIELD, g=10 cm

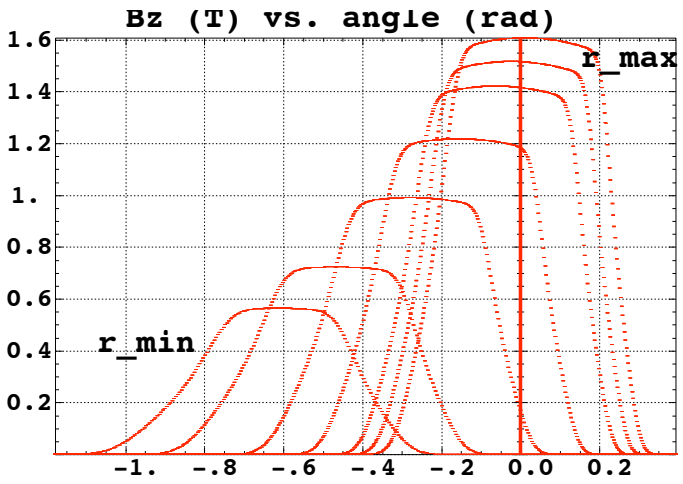

4.2 Paraxial tunes

A comparison between smooth approximation and stepwise ray-tracing

• **Working hypothesis :**

Spiral angle ξ = 52 degrees, field index k = 2.5

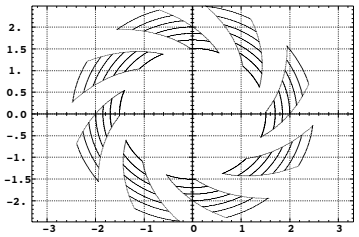

• **Smooth approximation data :**

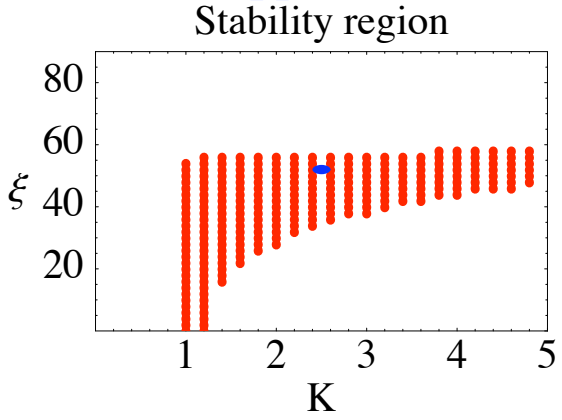

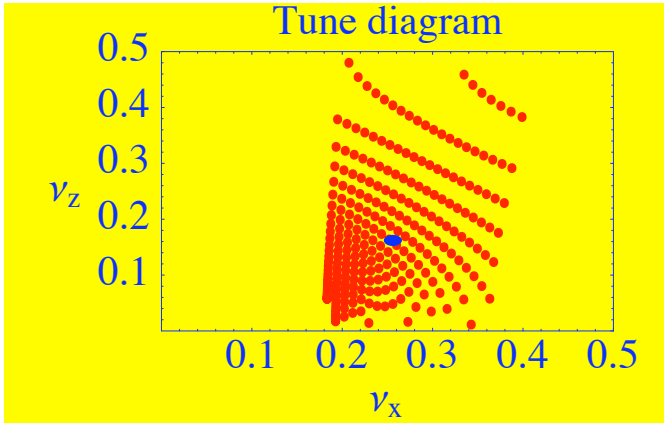

• **In the comparison Table, at the right, matrix method includes correction on R_{43} term for FF extent :**

$$\frac{\tan\epsilon}{\rho} \longrightarrow \frac{\tan(\epsilon-\psi)}{\rho}$$

with $\psi = \frac{g}{\rho} I_1 \frac{(1+\sin(\alpha)^2)}{\cos(\alpha)}$

wherein

$I_1 = \int_{-\infty}^{+\infty} \frac{B_Z(s)(B_0-B_Z(s))}{gB_0^2} ds\ \alpha\ \mathcal{L}_{FF}/g$

$\alpha = \epsilon - 1.2\frac{K_1 g}{\rho}$

g : gap size,

ρ **: bending radius, proportional to local** r **given that** $\rho\ \sin(\theta_F/2) = r\ \sin(A_F/2.)$

E (MeV)	parallel gap ν_X	parallel gap ν_Z	gap=$(g_0/r_0)\times r$ ν_X	gap=$(g_0/r_0)\times r$ ν_Z
Matrix method :				
3.55	0.263381	0.140956	0.263381	0.187253
7.96	0.263381	0.154776	0.263381	0.187253
21.0	0.263381	0.169278	0.263381	0.187253
42.6	0.263381	0.178731	0.263381	0.187253
69.4	0.263381	0.184814	0.263381	0.187253
85.	0.263381	0.187253	0.263381	0.187253
Ray-tracing method :				
3.55	0.256052	0.148243	0.257628	0.187178
7.96	0.256687	0.159290	0.257625	0.187190
21.0	0.257267	0.171474	0.257616	0.187203
42.6	0.257528	0.178861	0.257616	0.187211
69.4	0.257833	0.183917	0.257621	0.187217
85.	0.257921	0.185909	0.257619	0.187220

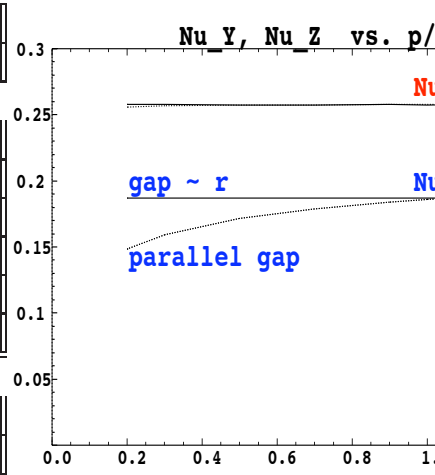

Conclusions :

(i) Excellent match on vertical focusing, when accounting for R_{34} correction

(ii) Some discrepancy ($\nu_{x,\text{Matrix}} - \nu_{x,\text{Ray-tracing}} \approx 5\,10^{-3}$) - effect of non constant r_{co} to be investigated.

4.3 Stability Limits

8 cells, K=2.5, ξ=52 deg

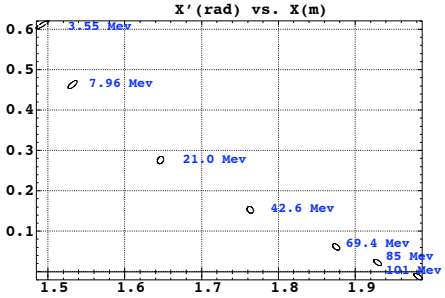

6 cells, K=1.6, ξ=44 deg

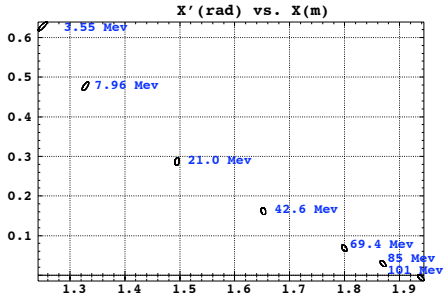

Step #1 : Search of closed orbit at various energies.

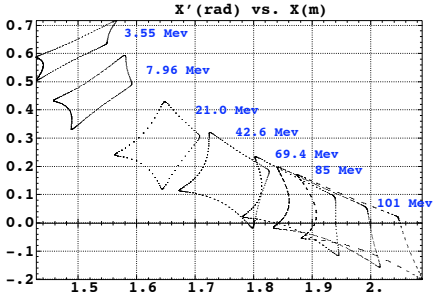

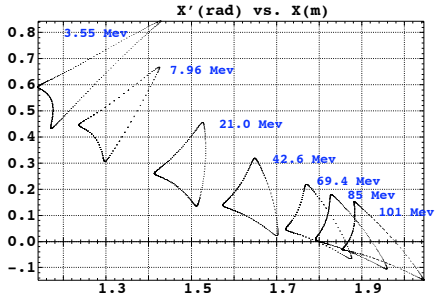

Step #2.a : Phase space at horizontal stability limit, z=0 .

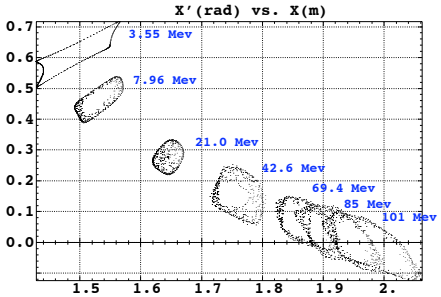

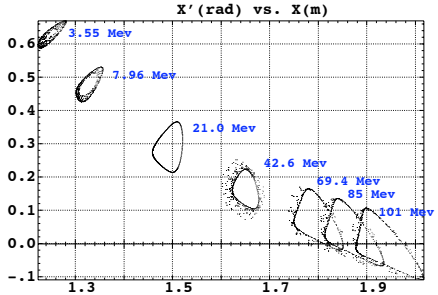

Step #2.b : Phase space at horizontal stability limit, z=ϵ .

8 cells case. Vertical phase space at vertical stability limit:
E = 3.55 , 7.96 , 21.96 , 42.57 , 69.40 and 85 MeV

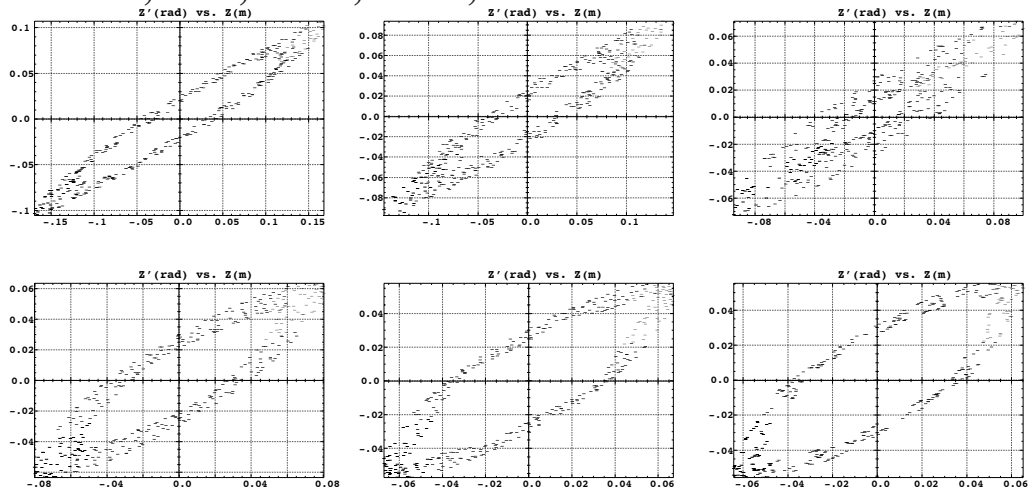

6 cells case. Vertical phase space at vertical stability limit:
E = 3.55 , 7.96 , 21.96 , 42.57 , 69.40 and 85 MeV

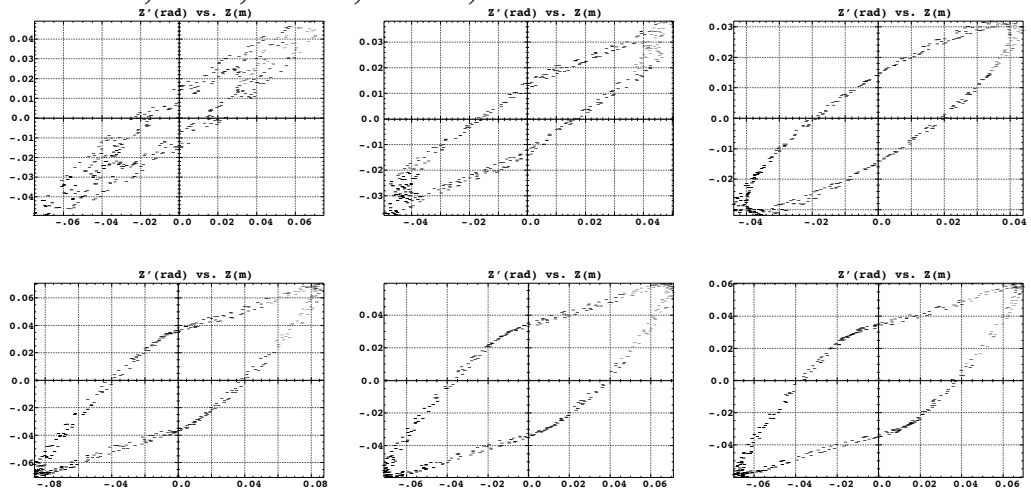

5 Conclusions

We are making all that automatic :

Starting from simple hypothesis, such as injection and extraction momenta, K, ξ, packing factor,

[• (0) Build field maps, e.g. 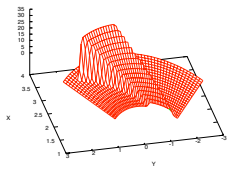 $\times M_K \times N_\xi$**]**

• (i) compute stability region in K/ξ and Qx/Qz diagrams, e.g., 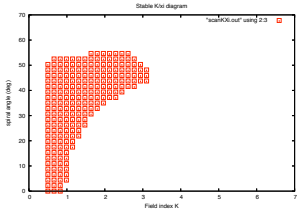 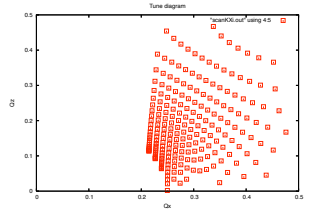 **, by**

(i.a) search of (r_{co}, r'_{co}), starting from theoretical values $(r\mathbf{max}\frac{\cos(\theta_F/2)}{\cos(\omega-\theta)})$, for a set of momenta,
(i.b) computation of paraxial tunes,

• scan working point region Qx/Qz for DA$_X$, DA$_Z$, over ΔK / $\Delta\xi$ range

For instance, ΔK can determine coil shaping parameters, whereas $\Delta\xi$ survey ascertains working region.

This is under developement.

Such tool can be benchmarked by 3-D magnet code computations.

In additon to machine design, it is expected to provide better understanding of beam dynamics properties.